A MATHEMATICAL MODEL OF A CRANKCASE SCAVENGED, TWO-STROKE, SPARK IGNITED ENGINE AND COMPARISONS WITH EXPERIMENTAL DATA

Richard R. Booy
Outboard Marine Corporation, Research Center
Milwaukee, Wisconsin

Roger B. Krieger
Institut Francais du Petrole
Paris, France

P. S. Myers and O. A. Uyehara
University of Wisconsin
Madison, Wisconsin

Abstract

A detailed mathematical model of the thermodynamic events of a crankcase scavenged, two-stroke SI engine is described. Energy balances, mass continuity equations, the ideal gas law, and thermodynamic property relationships are combined to give a set of coupled ordinary differential equations which describe the thermodynamic states encountered by the engine systems during one cycle of operation. A computer program is used to integrate the equations, adjusting the initial estimates until the final conditions agree with the initial estimates, that is, until a cycle results. Experimental data from the simulated engine are compared with the computed results.

1. INTRODUCTION

Internal combustion engine design has been more an art than a science from the early designs back before the turn of the century right up to present day manufacture. Engine manufacturers with experience dating back to the beginnings of the industry still rely largely on cut and try methods to evaluate changes in engine design on engine performance. Besides being time consuming and costly, this method does not always permit complete isolation of the effect of changes to the variable under consideration from unintentional changes to other engine variables. For instance, in a study of the effect of varying gas transfer port locations in the cylinder walls of a two-stroke engine cylinder, invariably more than one cylinder block or liner will be required for the study. The subsequent teardown and rebuild of the engine with different parts will likely introduce changes in such variables as ring friction, bearing fits and part alignment that may obscure or at least alter the effect of the change to the variable under study.

Engine designers would welcome the opportunity to arrive at a new engine design or to evaluate changes to a given design with a faster and more accurate method than that of cut and try on the actual hardware. It was for this reason that a joint project was undertaken between Outboard Marine Corporation and the Mechanical Engineering Department at the University of Wisconsin to develop a mathematical model of a crankcase scavenged, spark ignited, two-stroke-cycle engine cylinder. The development of an operating mathematical model for a single cylinder engine of this type became the subject of the

PhD thesis of Roger B. Krieger(1),*now at Institut Francais de Petrole in Paris. A subsequent parameter study using this model was performed by Vijay Sathe, now at Cooper Bessemer Corporation, and was the subject of his MS thesis (2).

2. MATHEMATICAL MODEL

2.1 COMPOSITE MODEL

The mathematical model for the simulation was derived by applying the equations of change to the systems to be studied. For this particular model, the three systems were (see Figure 1):

(1) The inlet system gases, bounded by the reed valves, the outer flow surface representing an air flow measuring device, and the inlet system walls,
(2) The crankcase system gases, bounded by the reed valves, the transfer ports and the crankcase and transfer passage walls, and
(3) The cylinder system gases, bounded by the transfer and exhaust ports, the cylinder sleeve, cylinder head and piston surfaces.

An exhaust system was not included in the model, and the condition of atmospheric exhaust was assumed.

The gases in each system were assumed to be in thermodynamic equilibrium and to behave as ideal gases at all times. The development of the mathematical model describing the thermodynamic behavior of the cylinder gases during the combustion portions of the cycle is described in reference 3. The development of the analogous equations for the cylinder gases during non-combustion periods and for the crankcase gases during both backflow and nonbackflow periods are analogous.

The method used involves the application of an energy balance to each system. This energy balance is then combined with thermodynamic property relationships, the mass continuity equation, and the differentiated ideal gas equation of state for the gases to yield an equation of the form

$$\frac{dT}{d\theta} = f_1(B_i, \theta) \qquad (1)$$

where:

T = Absolute temperature of the gas
B_i = Thermodynamic properties of the gas
θ = Engine crankangle position

The general procedure used to solve such an equation on a computer is to start at some value of θ, say θ_1, and obtain the value $T(\theta_1 + \Delta\theta)$ from the value $T(\theta_1)$ by adding to $T(\theta_1)$ some estimate of $T(\theta_1 + \Delta\theta) - T(\theta_1)$ based on some combination of value of f_1 evaluated at or near θ where $\theta_1 \leq \theta \leq \theta_{final}$.

The degree of approximation associated with any of the suitable numerical integration methods is partly related to the so-called truncation error of the method. This truncation error is sometimes determined by comparing the formula for the particular method with a Taylor series expansion about the same point (in this case θ) and observing the order of the first term in the Taylor series which does not have a matching term in the integration formula. Thus, if the integration formula has no term corresponding to the second derivative, the method would be said to have a truncation error of the order of $(\Delta\theta)^2$.

In choosing the integration method to be used in the simulation, one determining factor was that the solution to the governing differential equations includes periods of rapid change of the thermodynamic variables as well as periods of slow change. Therefore, it was desired to be able to adjust the integration step size, $\Delta\theta$, to keep the absolute truncation error more nearly constant during these various periods. The step size is most conveniently changed with the so-called "self-starting" methods which use only the present state variables and no previous values of these state variables. Due to the complexity of the actual function f_1 of equation (1), no attempt was made to estimate the truncation error to determine when periods of rapid change are encountered and the step size should be reduced. Rather, an iterative method was chosen such that whenever the difference between two successive approximations to the value of $T(\theta_1 + \Delta\theta)$ does not become less than some specified error tolerance within a specified number iterations, the step size, $\Delta\theta$, is reduced to 1/5 of its normal value for 5 $\Delta\theta$ steps. After the fifth reduced step, $\Delta\theta$ is set back to its original value.

The self-starting, iterative, numerical integration method used was that of Huen with iteration (4). This uses the Euler method to get a first approximation, called $T_1(\theta_1 + \Delta\theta)$, to the value of $T(\theta_1 + \Delta\theta)$. With this method

*Numbers in parenthese designate references at end of paper.

$$T_1(\theta_1 + \Delta\theta) = T(\theta_1) + \Delta\theta \cdot f_1(B_i(\theta_1), \theta_1) \quad (2)$$

Then the function f_1 of equation 1 is evaluated at $\theta_1 + \Delta\theta$ using the approximate values of the $B_i(\theta_1 + \Delta\theta)$ based on $T_1(\theta_1 + \Delta\theta)$ and $\theta_1 + \Delta\theta$. A corrected value of $T(\theta_1 + \Delta\theta)$ is then calculated using the formula of Huen, which is

$$T_2(\theta_1 + \Delta\theta) = T_1(\theta_1) + \Delta\theta/2\left[f_1(B_i(\theta_1), \theta_1) + f_1(B_i(\theta_1 + \Delta\theta), \theta_1 + \Delta\theta)\right] \quad (3)$$

The difference between approximations $T_2(\theta_1+\Delta\theta)$ and $T_1(\theta_1 + \Delta\theta)$ to the actual value of $T(\theta_1 + \Delta\theta)$ is compared to the specified error tolerance. If the difference is within the tolerance (normally 1%), the value of $T_2(\theta_1 + \Delta\theta)$ is accepted as the value of $T(\theta_1 + \Delta\theta)$, the program is indexed by causing $\theta_1 + \Delta\theta$ to assume the role of the new θ_1, and the solution method is then repeated for the next $\Delta\theta$ increment. If the difference is not within the tolerance, iteration is accomplished by causing the value of $T_1(\theta_1 + \Delta\theta)$ to be replaced by the value of $T_2(\theta_1 + \Delta\theta)$ and $f_1(B_i(\theta_1 + \Delta\theta), \theta_1 + \Delta\theta)$ is recalculated based on the new value for $T_1(\theta_1 + \Delta\theta)$. A new $T_2(\theta_1 + \Delta\theta)$ is then calculated using equation 3, and the subsequent difference again compared to the specified error tolerance. This procedure is repeated until the difference is within the error tolerance or the specified limit of iterations is reached. If the iteration limit is reached, the step size, $\Delta\theta$, is reduced as described previously.

Because a detailed analysis of the error in the solution resulting from the use of the integration method chosen would be extremely difficult even if the function f_1 of equation 1 were simple, an understanding of the physical processes which the simulation is intended to describe was extensively used to modify the integration step size during various portions of the cycle.

2.2. INDIVIDUAL MODELS

The simulation program includes several models, which will be described briefly.

Combustion. The model for cylinder combustion assumes the cylinder gases to be divided into one sub-system containing the burned gases and a second sub-system containing the unburned fresh charge. The combustion process is assumed to take place by transferring mass from the unburned system to the burned system according to some prescribed schedule. The amount of energy released in the form of heat is calculated for each increment of mass so transferred.

A number of simplifying assumptions are contained within this model, such as uniform pressure throughout the entire cylinder system containing both burned and unburned systems, no mixing or transfer of heat across the boundary between the two systems, each system in equilibrium and behaving as an ideal gas, and eventual complete transfer of mass from the unburned to the burned system.

Gas flow. Fluid flow models were derived for the gas flow through the various systems of the engine. Mass flow rates are calculated across the mass flow surfaces representing the air flow measuring element, the carburetor venturi, the reed valve inlet, the transfer ports and the exhaust ports.

Mass flow through the fixed restrictions, such as the flow element and the carburetor venturi, are calculated from the flow area and the statically measured flow coefficient for that restriction, and the pressure ratio across the restriction. For the flow surfaces with varying flow area, it was also necessary to derive some expression for the flow area and flow coefficient as a function of some other engine variable. In the case of the transfer and exhaust ports, area is only a function of engine geometry and engine crankangle. However, for the case of the reed valves, a separate model was used to calculate valve motion and resulting flow area.

Reed valve motion. The reed valve is shown in figure 2 and consists of a wedge shaped box with four openings on each face of the wedge. The openings are covered by metal reeds made of approximately 0.010 thick spring steel. The reed is not loaded in its closed position against the reed box. A reduction in crankcase pressure below that of the inlet system causes a pressure force on the portion of the reed covering the opening in the reed box, and the reed then opens into the crankcase permitting flow to occur. As the reed opens, the spring force and inertia force of the reed oppose its motion.

The reed valve model describes the motion of the tip of the reed as a function of the pressure, spring and inertia forces acting on the reed. The basis of the model was to devise a spring-mass system which had the same motion as the tip of the reed when equivalent forcing functions were applied to the reed and the lumped mass. A description of the assumptions made, the derivation of the model equations as well as a defense of its validity may be found in references 1 and 5.

Scavenging. The scavenge process in a two-stroke cycle engine is the gas exchange process whereby the residual products of combustion in the cylinder are displaced out through the exhaust ports by the incoming fresh charge being transferred

from the crankcase through the transfer ports into the cylinder. Ideally, all of the residual combustion products are expelled from the cylinder without loss of fresh charge either by mixing or short circuiting. In an actual engine, both mixing and short circuiting do occur to varying degrees, depending on engine design.

The scavenging process assumed by the simulation program is that of "perfect mixing". With this assumption, each increment of mass of fresh charge that enters the cylinder mixes completely and instantaneously with the mixture in the cylinder, and an equal amount of the mixture leaves the cylinder through the exhaust ports. The resulting scavenging efficiency from this process is close to actual scavenging efficiencies measured on many engines. The composition of the exhaust flow rate is adjusted by the simulation to follow a scavenging schedule specified in a subroutine to the main program. This subroutine can readily be changed to follow any scavenging schedule desired in place of that of perfect mixing.

Fuel vaporization. An arbitrary model is used to determine fuel vaporization rates in the simulation. A specified percentage (20%) of the fuel per cycle is assumed to vaporize in the inlet system between the carburetor and the reed valves. The remainder of the liquid fuel is assumed to vaporize completely in the crankcase before the end of the reed flow process. A continuous mass balance is used to determine the amount of liquid remaining at any instant. Then the vaporization rate per crank angle degree at each crank angle increment is computed by dividing the mass of liquid fuel remaining at that increment by the total number of crank angle degrees remaining until the specified end of vaporization. Although the specified end of the vaporization process may differ from that of the actual engine, preliminary calculations indicate that the duration of vaporization is not a major variable in the simulation.

Heat transfer. The inlet system is considered adiabatic; the only heat transfer calculation made for this system is that for the vaporization of liquid fuel. The heat transfer surfaces in the crankcase system are the piston underside, the lower portion of the cylinder sleeve, the crankcase walls, the transfer passage walls and the transfer passage cover plate. The heat transfer surfaces in the cylinder system are the cylinder head, the upper portion of the cylinder sleeve and the piston crown. Each heat transfer surface is assumed to be at one uniform temperature for the cycle. At the end of each cycle, a one-dimensional heat transfer rate balance is performed on each surface to determine better estimates of the gas side surface temperatures for the next cycle iteration. The Eichelberg (6) correlation is used in the simulation for the gas side heat transfer coefficient in both the cylinder and the crankcase. A correlation for the average coolant side heat transfer coefficient was developed from experimental data from the test engine and used in the simulation in the heat transfer rate balance calculations.

2.3 SEQUENCE OF OPERATIONS

A very brief description of the sequence of operations within the simulation will be given as an aid in understanding program operation. This description covers only the logic aspects in proceeding from state to state through the cycle for the systems involved, and does not include a discussion of the initial inputing of data nor any data output.

First, all energy subroutines are called to calculate the thermodynamic properties at state 1 for each system.

Second, heat transfer rates are calculated for the cylinder and crankcase systems. For the cylinder system, heat transfer rates are calculated for both the burned and the unburned systems during combustion. For the crankcase system, separate rates are calculated for both the backflow gas system and the fresh charge system during periods of backflow.

Third, mass flow rates are calculated for each system as a function of exhaust and transfer port openings, if any. Mass flow rate through the reed valves is calculated for normal or backflow if there is any reed valve opening. State 2 inlet system properties are also calculated, as are fuel vaporization rates in the various systems.

Fourth, thermodynamic mixture properties for the cylinder system are calculated and flow enthalpies specified for each system for the various flow alternatives of direction and composition.

Fifth, the rates of change of total mass and mass fractions are calculated for each system.

Sixth, the temperature derivative expressions (equation 1) are assembled for the various systems for combustion or non-combustion and for normal flow or backflow.

Seventh, the Euler estimates are computed for the properties of the various systems at state 2 using the values at state 1, the rate of change of

the values at state 1 and the time increment for the change to state 2.

The program next repeats the previous steps to obtain derivatives at state 2 and then uses the method of Huen to obtain better estimates of the state 2 properties, called state 3 properties. The state 3 properties are used as new estimates to the state 2 properties until state 3 and state 2 properties are within 1% agreement. The program then indexes with the new state 1 properties becomming the state 3 properties, and all previous calculations are repeated.

The program was written in FORTRAN 63 and run on a CDC 3600 digital computer at the University of Wisconsin. The program with subroutines is about 2500 cards long in FORTRAN and about 1430 cards long in pre-compiled binary. Compilation time of the FORTRAN decks is approximately seven minutes. Execution times for one cycle requires about 1 1/2 minutes and the simulation converges in 5 to 7 cycle iterations with reasonable initial estimates.

3. VERIFICATION OF RESULTS

Data generated by the simulation program were compared to experimental data taken from a single cylinder engine constructed by modifying a former production V-4 90 hp outboard motor powerhead, manufactured by Outboard Marine Corporation. The engine was run on a dynamometer with suitable means for measuring engine speed and load, air flow, fuel flow, cooling water flow, and significant metal surface temperatures and instantaneous gas pressures within the engine during its operation. Test data were taken at engine speeds from 2500 to 5000 rpm. An external blower was used on some runs to make up the pressure loss across the inlet air flow measuring equipment.

Figures 3 and 4 show predicted reed valve motion as a function of engine crank angle and engine speed. While there is no experimental data for quantitative comparisons, high speed movies taken from downstream of the reed in an operating engine at wide open throttle indicated the same qualitative behavior as that in figure 3.

Total engine air flow from experimental data and from the simulation is shown in figure 5 for operation both with and without the make-up blower. This parameter is naturally greatly affected by reed valve motion.

Computed instantaneous cylinder, crankcase and carburetor system pressures vs. engine crank angle are plotted in figures 6 and 7 for 2500 and 4500 rpm. These may be compared to oscillograms from the test engine at the same speeds, shown in figures 8 and 9 respectively.

The calculated values of brake horsepower vs. engine speed from the simulation are compared in figure 10 to the experimental values for operation both with and without the make-up blower on the inlet system. The calculated values of brake horsepower were obtained by subtracting experimentally determined values of friction horsepower (from motored data) from the simulation calculated values of indicated horsepower.

Similar comparisons were made between numerous other experimental and calculated values such as brake specific fuel consumption, brake thermal efficiency, peak cylinder pressures, cylinder trapped fresh mass and scavenging efficiency, heat loss per cycle to coolant, and engine metal surface temperatures.

4. CONCLUSIONS

Based on the comparisons with experimental data, the simulation appears to describe satisfactorily the wide open throttle behavior of the test engine for the speed range of 2500-5000 rpm. Additional experimental data for accurate average cylinder pressures, cylinder scavenging schedules during a cycle, and reed valve displacement-time data with corresponding pressures across the reed would be valuable aids to improve the simulation model.

REFERENCES

1. Krieger, R.B., "The Simulation of a Two-Cycle, Crankcase Scavenged, Spark Ignition Engine on a Digital Computer and Comparison of Results with Experimental Data", PhD Thesis, University of Wisconsin, 1968.
2. Sathe, V.V., "Parametric Studies Using a Mathematical Model of a Two-Stroke-Cycle Spark Ignition Engine", M.S. Thesis, University of Wisconsin, 1969.
3. Krieger, R.B. and Borman, G.L., "The Computation of Apparent Heat Release for Internal Combustion Engines", ASME Paper No. 66-WA/DGP-4, 1966.
4. Henrici, P., "Discrete Variable Methods in Ordinary Differential Equations", John Wiley and Sons, Inc., New York, 1964.
5. Krieger, R.B., Booy, R.R., Myers, P.S. and Uyehara, O.A., "Simulation of a Crankcase Scavenged, Two-Stroke, SI Engine and Comparisons with Experimental Data", SAE Paper690135, Jan. 1969.

6. Eichelberg, G., "Some New Investigations of Old Internal Combustion Engine Problems", Engineering, Vol. 148-149, 1939.

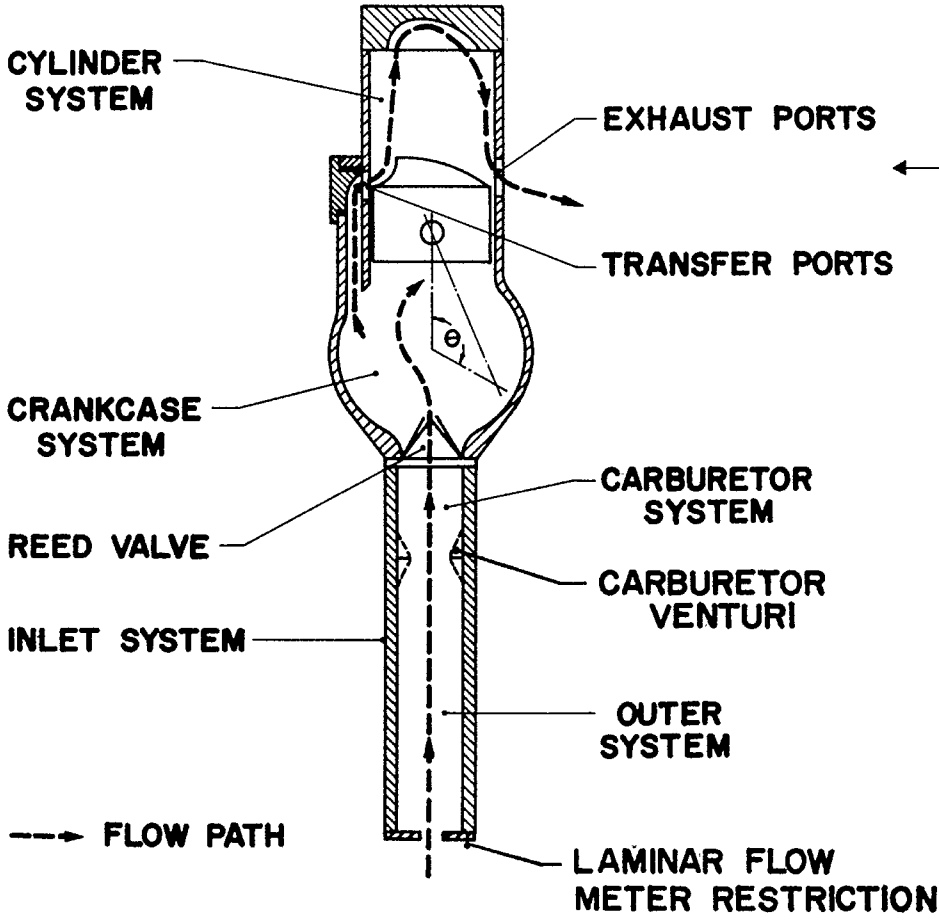

FIG. 1 SYMBOLIC CUT-AWAY OF SIMULATED ENGINE.

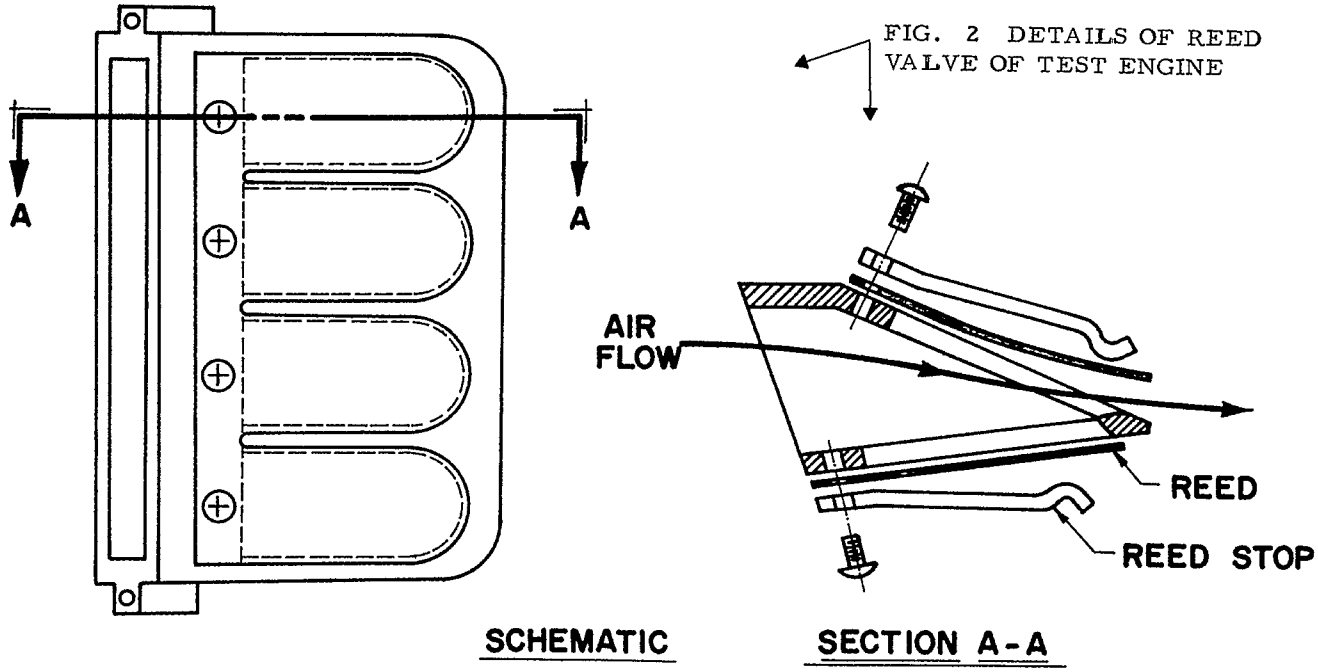

FIG. 2 DETAILS OF REED VALVE OF TEST ENGINE

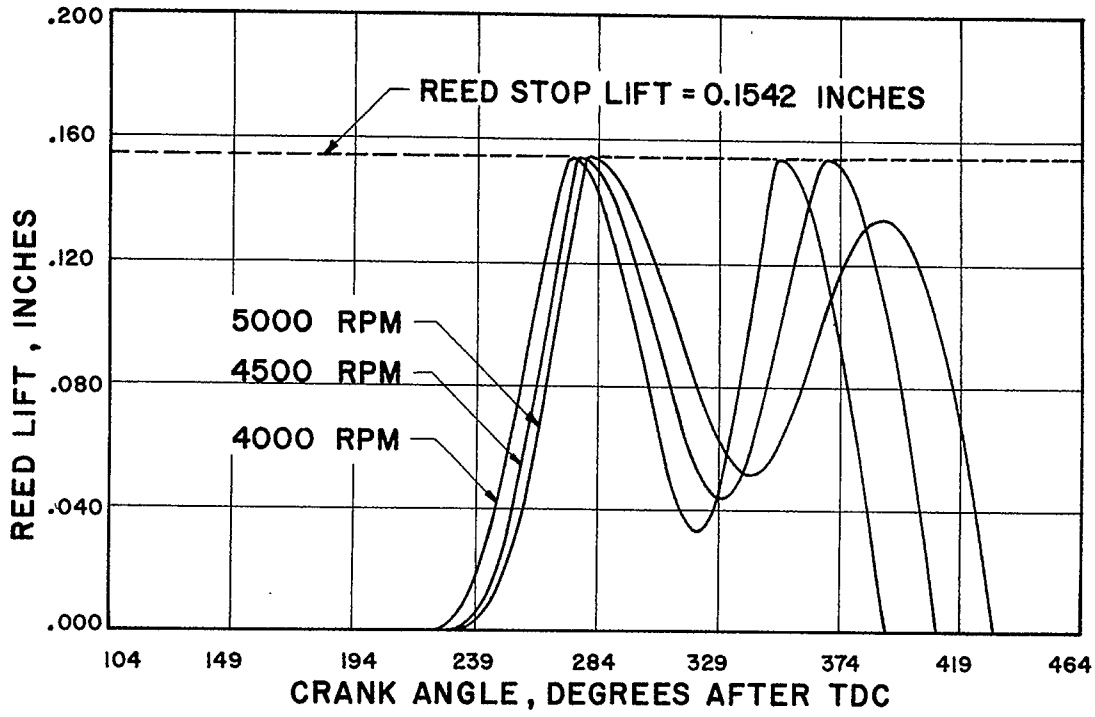

FIG. 3 COMPUTED REED LIFT VERSUS CRANKANGLE FOR 4000, 4500, AND 5000 RPM.

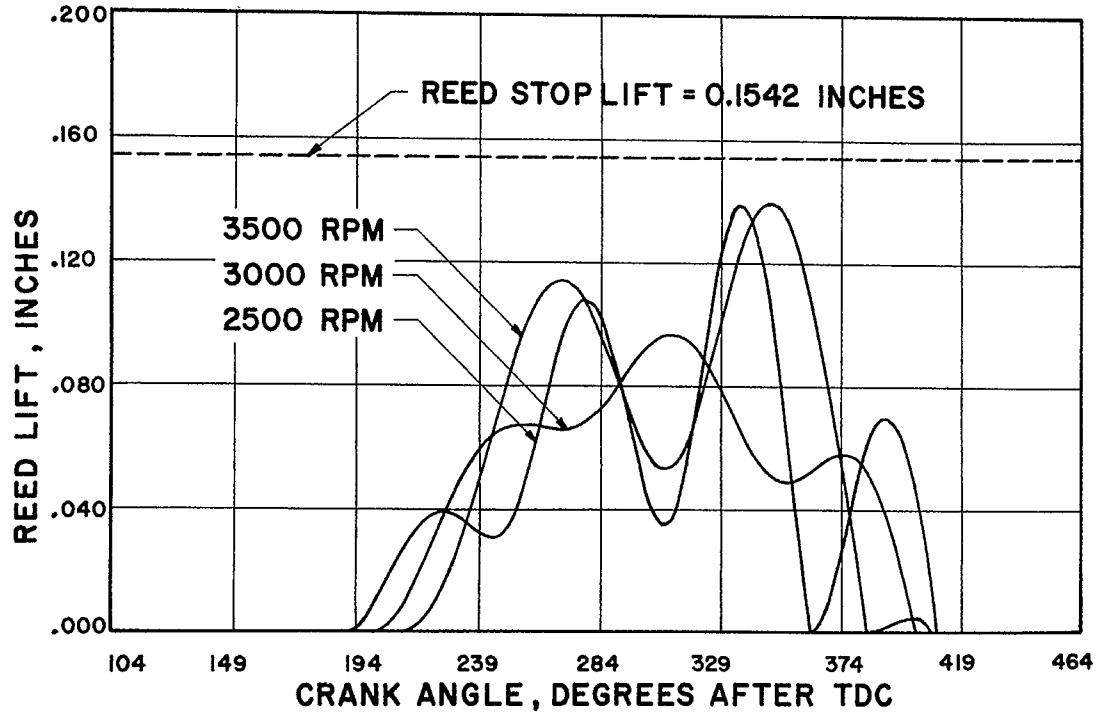

FIG. 4 COMPUTED REED LIFT VERSUS CRANKANGLE FOR 2500, 3000, and 3500 RPM.

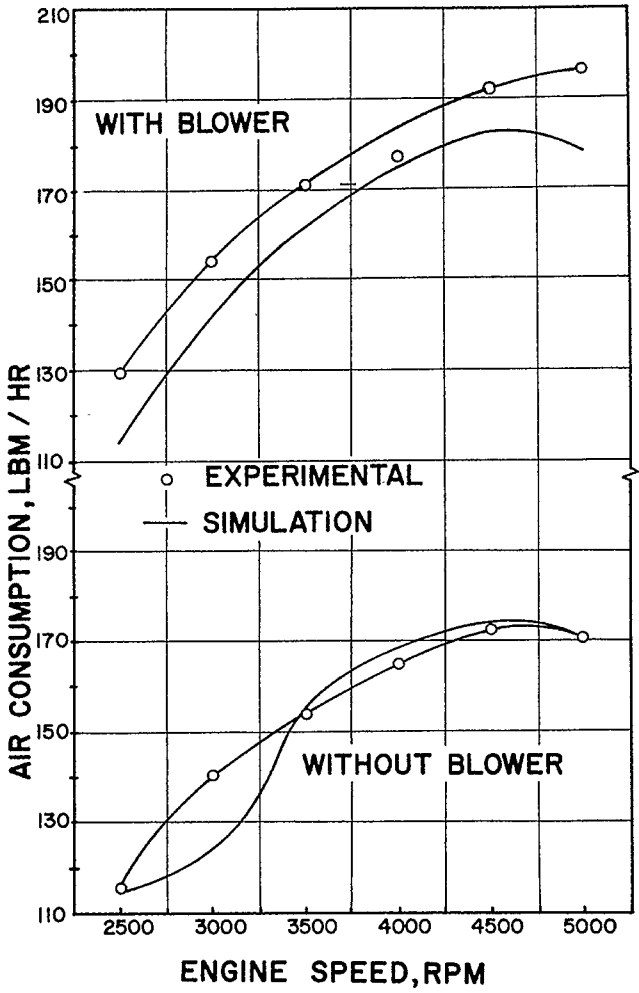

FIG. 5 EXPERIMENTAL AND COMPUTED AIR FLOW VERSUS ENGINE SPEED FOR OPERATION WITH AND WITHOUT BLOWER.

FIG. 6 COMPUTED CYLINDER, CRANKCASE, AND CARBURETOR SYSTEM PRESSURE VERSUS CRANKANGLE FOR 2500 RPM WITH BLOWER.

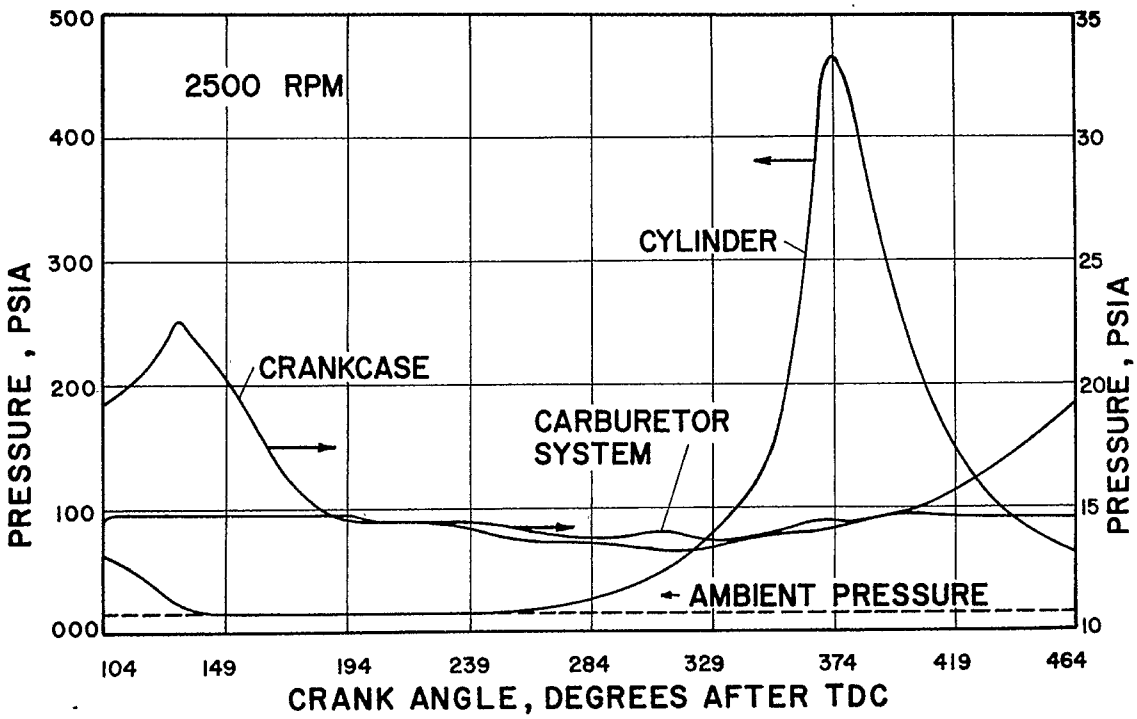

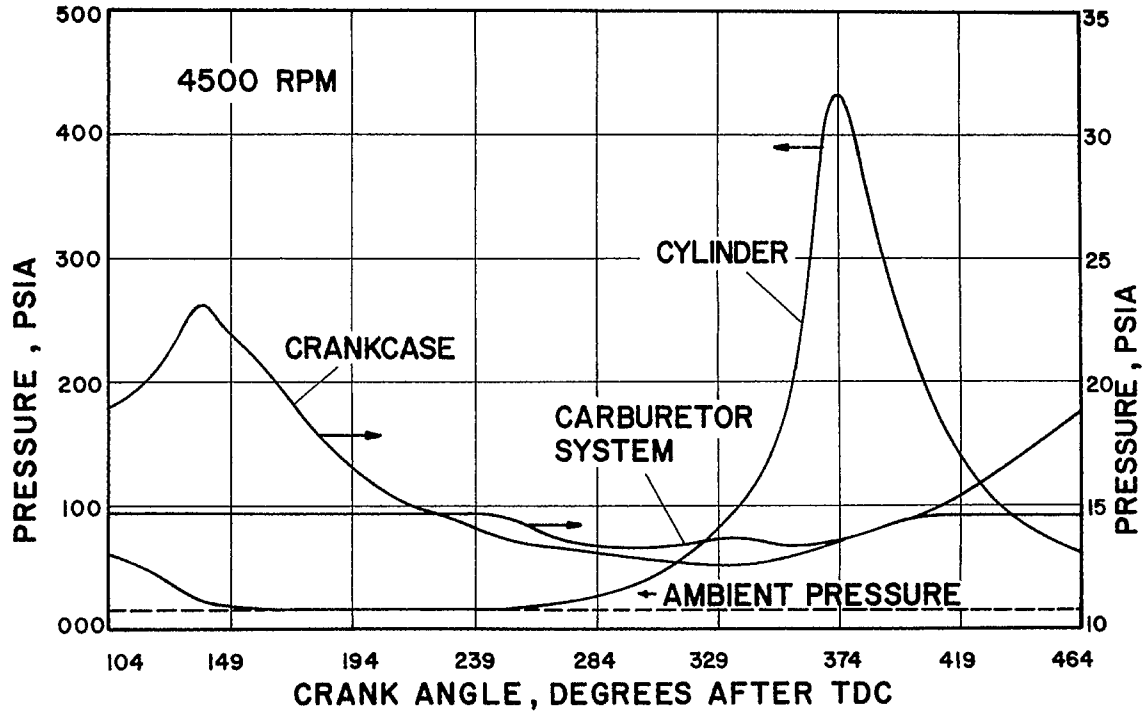

FIG. 7 COMPUTED CYLINDER, CRANKCASE, AND CARBURETOR SYSTEM PRESSURE VERSUS CRANKANGLE FOR 4500 RPM WITH BLOWER.

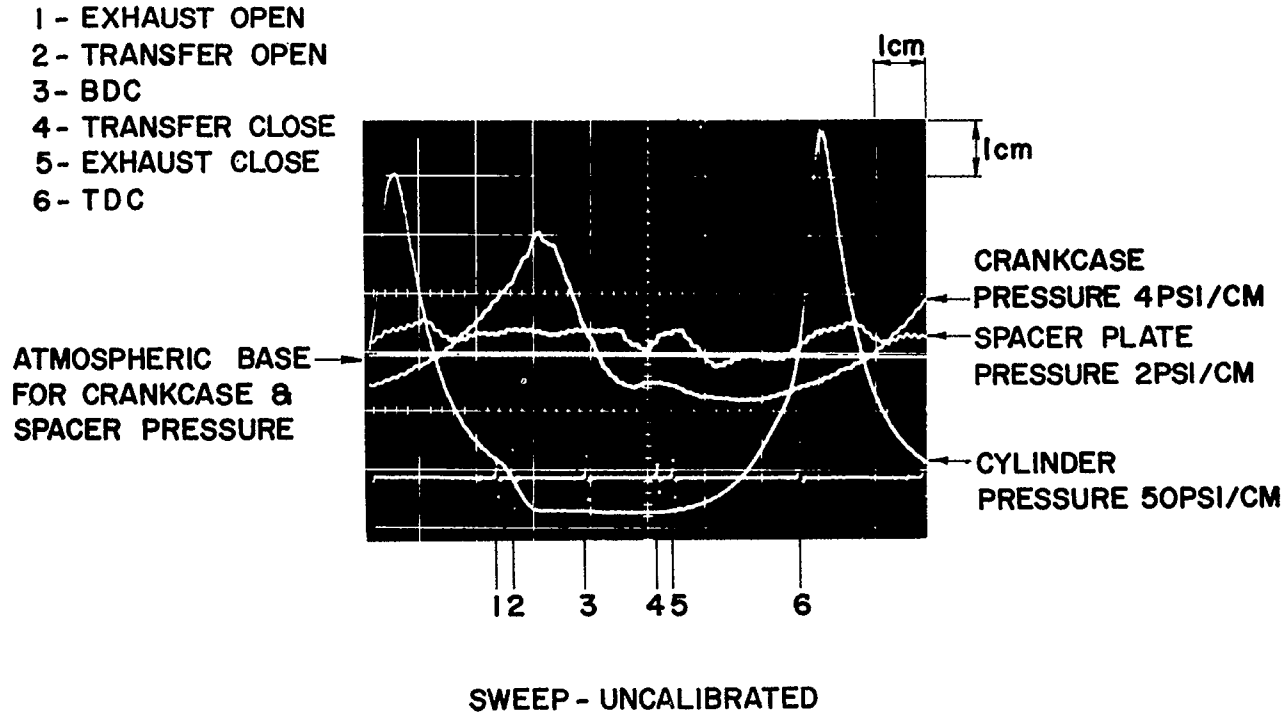

FIG. 8 OSCILLOSCOPE TRACE OF CYLINDER PRESSURE, CRANKCASE PRESSURE, AND SPACER PLATE PRESSURE FROM TEST ENGINE VERSUS CRANKANGLE. 2500 RPM WOT WITH BLOWER USED TO RECOVER MERIAM MEASURING ELEMENT PRESSURE LOSS.

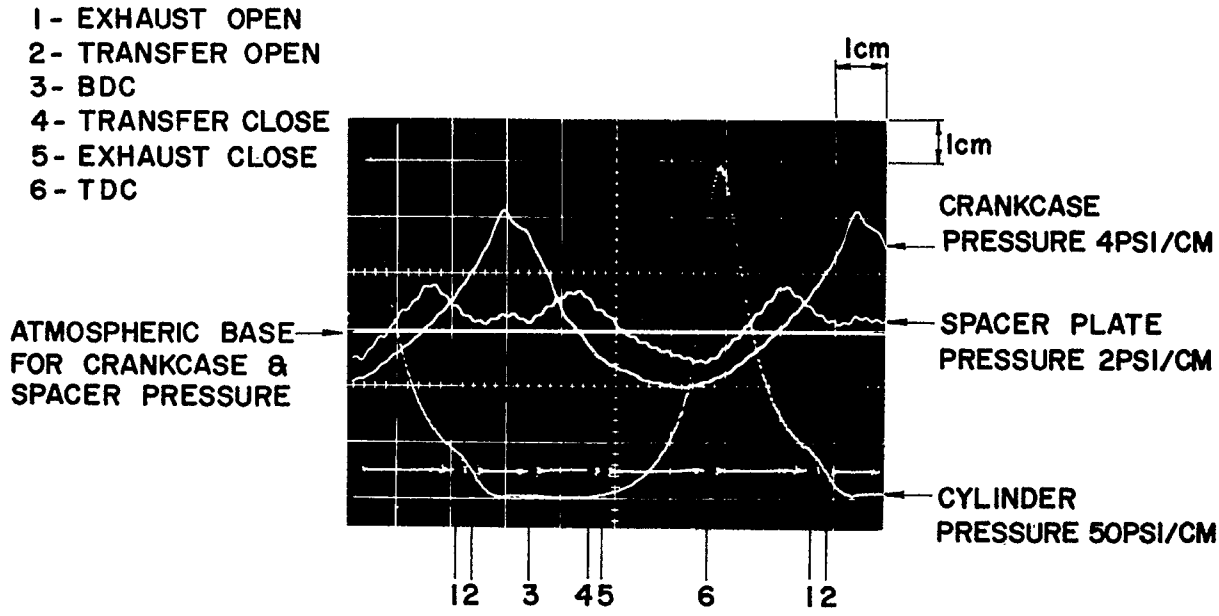

FIG. 9 OSCILLOSCOPE TRACE OF CYLINDER PRESSURE, CRANKCASE PRESSURE, AND SPACER PLATE PRESSURE FROM TEST ENGINE VERSUS CRANKANGLE. 4500 RPM WOT WITH BLOWER USED TO RECOVER MERIAM MEASURING ELEMENT PRESSURE LOSS.

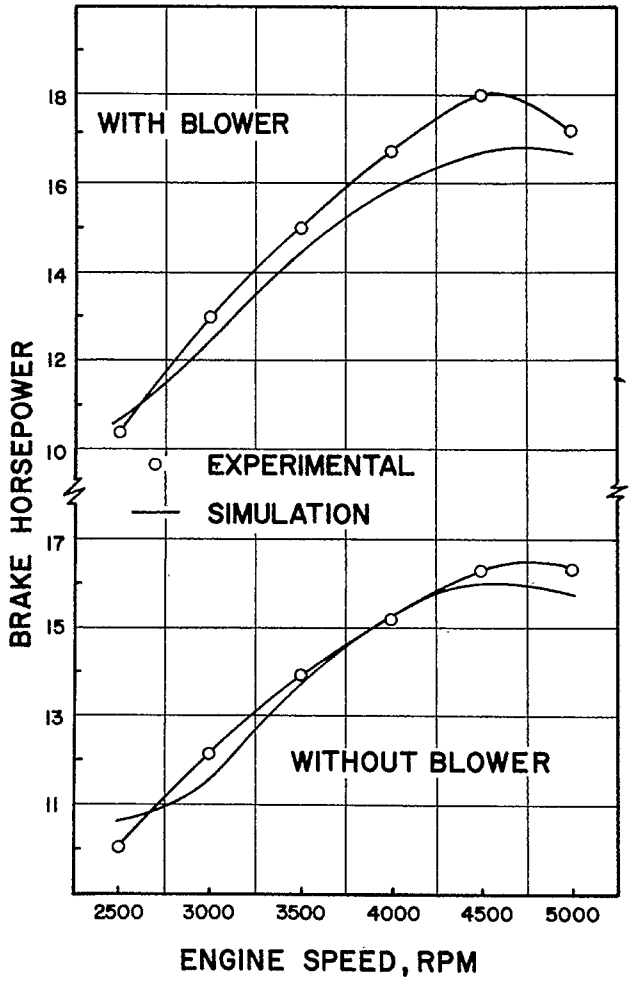

FIG. 10 COMPUTED AND EXPERIMENTAL BRAKE HORSEPOWER VERSUS ENGINE SPEED FOR OPERATION WITH AND WITHOUT BLOWER.